THE JOURNAL OF BIOLOGICAL CHEMISTRY VOL. 284, NO. 33, pp. 22123–22132, August 14, 2009

Identification of a Disulfide Bridge Essential for Transport Function of the Human Proton-coupled Amino Acid Transporter hPAT1*

Received for publication, May 21, 2009, and in revised form, June 19, 2009 Published, JBC Papers in Press, June 23, 2009, DOI 10.1074/jbc.M109.023713

Madlen Dorn[‡§], Matthias Weiwad[¶], Fritz Markwardt[‖], Linda Laug[§], Rainer Rudolph[‡], Matthias Brandsch[§], and Eva Bosse-Doenecke[‡1]

From the [‡]Institute of Biochemistry/Biotechnology, Faculty of Science I and [§]Biozentrum, Martin-Luther-University Halle-Wittenberg, D-06120 Halle, the [¶]Max-Planck Research Unit-Enzymology of Protein Folding, Weinbergweg 22, D-06120 Halle, and the [‖]Julius-Bernstein-Institute for Physiology, Faculty of Medicine, Martin-Luther-University Halle-Wittenberg, D-06097 Halle, Germany

The proton-coupled amino acid transporter 1 (PAT1, SLC36A1) mediates the uptake of small neutral amino acids at the apical membrane of intestinal epithelial cells after protein digestion. The transporter is currently under intense investigation, because it is a possible vehicle for oral drug delivery. Structural features of the protein such as the number of transmembrane domains, the substrate binding site, or essential amino acids are still unknown. In the present study we use mutagenesis experiments and biochemical approaches to determine the role of the three putative extracellular cysteine residues on transport function and their possible involvement in the formation of a disulfide bridge. As treatment with the reducing reagent dithiothreitol impaired transport function of hPAT1 wild type protein, substitution of putative extracellular cysteine residues Cys-180, Cys-329, and Cys-473 by alanine or serine was performed. Replacement of the two highly conserved cysteine residues Cys-180 and Cys-329 abolished the transport function of hPAT1 in *Xenopus laevis* oocytes. Studies of wild type and mutant transporters expressed in human retinal pigment epithelial (HRPE) cells suggested that the binding of the substrate was inhibited in these mutants. Substitution of the third putative extracellular nonconserved cysteine residue Cys-473 did not affect transport function. All mutants were expressed at the plasma membrane. Biotinylation of free sulfhydryl groups using maleimide-PEG_{11}-biotin and SDS-PAGE analysis under reducing and nonreducing conditions provided direct evidence for the existence of an essential disulfide bond between Cys-180 and Cys-329. This disulfide bridge is very likely involved in forming or stabilizing the substrate binding site.

The solute carrier (SLC)[2] superfamily represents the second largest group of membrane proteins after the G-protein-coupled receptor (GPCR) superfamily in the human genome. Comprising 384 members, the 46 SLC families include transporters for inorganic ions, amino acids, neurotransmitters, sugars, purines, fatty acids, and other substances (1). Ten SLC families contain 47 known transporters for amino acids and 48 related orphan transporters. Phylogenetic analysis revealed four main clusters (α, β, γ, and δ). Together with members of the SLC32 and SLC38 families, the proton-coupled amino acid transporter 1 (PAT1) was placed into group β. PAT1 is a member of the SLC36 family (SLC36A1). It was originally identified as the lysosomal amino acid transporter (LYAAT1) in rat brain (2). Subsequently, mouse and human homologs were cloned from mouse intestine (3) and from Caco-2 cells (4), respectively. PAT1 is identical to the H^+/amino acid cotransporter that has been functionally described in Caco-2 cells (5). It is localized mainly to the apical membrane of intestine epithelial cells and is also found in lysosomes in brain neurons (4) facilitating the transport of amino acids from luminal protein digestion or lysosomal proteolysis, respectively. The transport of substrates via PAT1 is driven by an inwardly directed H^+ gradient. Recently we could identify the conserved His-55 as being responsible for binding and translocation of the proton (6).

Prototypic substrates for PAT1 are small neutral amino acids (*e.g.* L-proline, glycine, β-alanine) and amino acid derivatives (*e.g.* γ-aminobutyric acid (GABA), α-(methylamino)-isobutyric acid) (3–5, 7–10). Recently, PAT1 gained much interest because it transports pharmaceutically relevant compounds such as D-cycloserine, L-azetidine-2-carboxylic acid, 3-amino-1-propanesulfonic acid, 3,4-dehydro-L-proline, vigabatrin, and other GABA analogs (8, 10, 11) rendering it an interesting target for the pharmaceutical industry. PAT1 seems to be one of the most important drug transporters in the intestine allowing oral availability of GABA-related and other drugs and prodrugs. Furthermore, a recent report shows involvement of this transporter family, namely the PAT2 subtype, in the autosomal dominant inherited disorder iminoglycinuria (12).

Unfortunately, up to now the exact three-dimensional structure of PAT1, the transmembrane domain topology, and the substrate binding site are unknown. More structural information of PAT1 would allow a better understanding of the molecular mechanisms of its function and drug interaction, which is so far being investigated only in classic transport studies. Mutational analysis of putative extracellular regions is a suitable tool

* This work was supported by the State Saxony-Anhalt Life Sciences Excellence Initiative Grant XB3599HP/0105T (to M. B. and E. B.-D.).

[1] To whom correspondence should be addressed: Inst. of Biochemistry/Biotechnology, Faculty of Science I, Martin-Luther-University Halle-Wittenberg, Kurt-Mothes-Str. 3, D-06120 Halle, Germany. Tel.: 49-345-5524934; Fax: 49-345-5527013; E-mail: eva.bosse-doenecke@biochemtech.uni-halle.de.

[2] The abbreviations used are: SLC, solute carrier; ABC transporter, ATP-binding cassette transporter; DTT, dithiothreitol; EL, extracellular loop; GABA, γ-aminobutyric acid; GPCR, G-protein-coupled receptor; HA, hemagglutinin; HRPE, human retinal pigment epithelium; IU, infectious units; PEG, polyethylene glycol; PAT1, proton-coupled amino acid transporter 1; MES, 4-morpholineethanesulfonic acid; PBS, phosphate-buffered saline; BSA, bovine serum albumin.

to get the first clue into transmembrane organization and relevant amino acid residues (6). This approach should also elucidate the spatial organization of the extracellular loops. The present study was performed to identify functionally important extracellular cysteine residues and their involvement in disulfide bridges. The relevance of disulfide bonds for membrane protein function is mainly based on the stabilization of a proper three-dimensional structure. The correct conformation in turn is essential for trafficking, surface expression, stability, and transport function. So far, intramolecular disulfide bonds have been identified for only very few SLCs, *e.g.* the serotonin transporter SERT and the dopamine transporter DAT (13–15). Native disulfide bonds are probably required for transporter function of the Na^+/glucose cotransporter SGLT1 (16, 17). For the type IIa sodium/phosphate cotransporter, it was shown that cleavage of disulfide bonds results in conformational changes that lead to internalization and subsequent lysosomal degradation of the transport protein (18). A similar stabilizing effect of an intramolecular disulfide bridge was also reported for the human ATP-binding cassette (ABC) transporter ABCG2 (19).

Linkage via cysteine residues can also be necessary for transporter oligomerization. For the rat serotonin transporter SERT (20) and for the human ABC transporter ABCG2 (21), intermolecular disulfide bridges could be identified. For the hexose transporter GLUT1, an intramolecular disulfide bond promotes tetramerization of the transporter (22, 23). On the other hand, removal of cysteine residues can also lead to an impaired trafficking and mislocalization of the transporter protein without a disulfide bridge being involved (13, 24, 25). In those cases, the cysteine residues themselves are assumed to play an important role for the trafficking and targeting of the transporter to the cell surface. Similarly, for several transporters, cysteine residues located in a transmembrane domain play a key role in substrate recognition. Single cysteines have been found to be essential for substrate binding of the rat organic cation transporters rOCT1 and rOCT2 (26) and the multidrug and toxin extrusion transporter MATE1 (27). The relevance of conserved cysteines for the integrity of a membrane protein has therefore to be investigated very thoroughly. Several earlier studies reported loss of function in cysteine mutants without testing membrane localization.

After assessing a negative influence of the reducing reagent DTT on hPAT1 function, we performed systematic mutagenesis in this study. The three putative extracellular cysteine residues Cys-180, Cys-329, and Cys-473 were individually exchanged to either alanine or serine residues. The resulting mutants were analyzed for substrate binding and transport in human retinal pigment epithelial (HRPE) cells and electrogenic transport in *Xenopus laevis* oocytes. Biochemical approaches provided direct evidence for an essential disulfide bond between Cys-180 and Cys-329. A triple mutant was constructed and examined to exclude other juxtamembrane cysteine residues as potential partners for disulfide bridges. The data suggest that this disulfide bridge is involved in forming or stabilizing the putative substrate-binding pocket. In addition, our results strongly support the eleven transmembrane domain topology model of hPAT1. This is consistent with our recently published data on glycosylation of hPAT1 (28).

EXPERIMENTAL PROCEDURES

Materials—L-[^{3}H]Proline (specific radioactivity 49 Ci/mmol) was purchased from GE Healthcare (Little Chalfont, UK). Chemical reagents were from Sigma. Cell culture media and supplements were obtained from Invitrogen (Karlsruhe, Germany). The following antibodies were used: polyclonal rabbit anti-HA tag antibody (Sigma), monoclonal mouse anti-HA tag antibody, goat anti-mouse horseradish peroxidase-conjugated antibody (Santa Cruz Biotechnology, Inc., Heidelberg, Germany) and AlexaFluor® 488 goat anti-rabbit antibody (Invitrogen). The recombinant modified vaccinia virus Ankara was provided by the GSF-Institute for Molecular Virology (Munich, Germany). Maleimide-PEG_{11}-Biotin was purchased from Pierce.

Construction of pNKS-HA-hPAT1 and pNKS-hPAT1—The *X. laevis* oocyte expression vector pNKS was kindly provided by Prof. G. Schmalzing (RWTH, Aachen, Germany) as pNKS-transducin. This vector contains the 5′- and 3′-untranslated regions of the *X. laevis* oocyte β-globin gene and the cDNA of murine transducin. The latter was cut out of the vector using the restriction enzymes AatII and XbaI. To clone the transporter cDNA into pNKS, AatII and XbaI restriction sites were introduced at the 5′- and 3′-end by PCR, respectively. As template, the previously described wild type cDNA of human PAT1 containing an N-terminal HA tag in the pSPORT1 (pSPORT1-HA-hPAT1) vector was used (6). For the analog construction of pNKS-hPAT1, the pSPORT1-hPAT1 served as template. After restriction enzyme digestion, the PCR product was ligated into the digested pNKS vector. The insertion of the correct cDNA was verified by sequencing.

Site-directed Mutagenesis—Cysteine residues at positions 180, 329, and 473 were exchanged for alanine and serine residues, respectively, with the QuikChange® II Site-directed Mutagenesis kit (Stratagene, La Jolla, CA). For expression in HRPE cells or *X. laevis* oocytes the pSPORT1-HA-hPAT1 vector (6) and the pNKS-HA-hPAT1 vector were used as template, respectively. Primers to introduce the desired mutations into the respective vector were as follows: (C180A) 5′-GGGACCACCAATAAC*GCC*CACAACAATGAGACGG-3′, (C180S) 5′-CCAATGGGACCACCAATAAC*AGC*CACAACAATGAGACG-3′, (C329A) 5′-CCCTCAACCTGCCCAAC*GCA*TGGCTGTACCAGTCAGTTAAG-3′, (C329S) 5′-CCCTCAACCTGCCCAAT*TCA*TGGCTGTACCAGTCAGTTAAG-3′, (C473A) 5′-CCATCTTCATCAATTCCACC*GCT*GCCTTCATATAGGG-3′, (C473S) 5′-CCATCTTCATCAATTCCACC*AGT*GCCTTCATATAGGG-3′. The insertion of the mutation and the correct cDNA sequence were confirmed by DNA sequencing (MWG Biotech AG, Ebersberg, Germany).

In Vitro cRNA Synthesis—The wild type and mutant pNKS-HA-hPAT1 and pNKS-hPAT1 constructs served as templates for cRNA synthesis. After linearizing the plasmids with NotI, cRNAs were synthesized using the mMESSAGE mMACHINE® SP6 kit (Ambion, Huntingdon, UK). The cRNAs were purified with the aid of the MEGAclear™ kit (Ambion), and the concentration was determined by UV absorbance at 260 nm. The cRNA was stored at −80 °C.

Cell Culture and Transfection—Human retinal pigment epithelial (HRPE) cells were grown in Dulbecco's modified Eagle's medium/F12 supplemented with 10% fetal bovine serum (Biochrom, Berlin, Germany) and 1% penicillin/streptomycin (Invitrogen) as described previously (6). Cells were transiently transfected with wild type and mutant pSPORT1-HA-hPAT1 using the modified vaccinia virus Ankara (MVA) (4, 29) and the Nanofectin® technology (PAA Laboratories, Cölbe, Germany) as reported by Metzner *et al.* (6). Briefly, HRPE cells grown in 24-well plates (Sarstedt, Nümbrecht, Germany) were infected 22 h after seeding with the recombinant MVA (50 IU/cell). After 30 min, cells were transfected with wild type and mutant HA-hPAT1 plasmid or the empty vector pSPORT1 as control. 21 h after transfection uptake measurements or immunofluorescence experiments were performed.

Uptake Measurements in Transfected HRPE Cells—Transfected cells were rinsed twice with uptake buffer (25 mM MES/Tris pH 6.0, 140 mM NaCl, 5.4 mM KCl, 1.8 mM $CaCl_2$, 0.8 mM $MgSO_4$, 5 mM glucose) at room temperature followed by incubation in uptake buffer containing 20 nM L-[^{3}H]proline for 10 min. Cells were washed four times with ice cold uptake buffer and solubilized in 500 μl of lysis buffer (0.2 M NaOH, 1% SDS). Scintillation mixture (2.8 ml) was added to each lysate, and the radioactivity was quantified by liquid scintillation spectrometry (Tri-Carb 2100TR, Packard Instrument Company, Meriden). To study the effect of DTT (Applichem, Darmstadt, Germany) treatment on L-[^{3}H]proline uptake, transfected cells were incubated for 20 min at room temperature in DTT-containing buffer (25 mM HEPES/Tris, pH 7.5, 140 mM NaCl, 5.4 mM KCl, 1.8 mM $CaCl_2$, 0.8 mM $MgSO_4$, 5 mM glucose, 10 mM DTT). Uptake experiments were carried out as described above except that the uptake buffer also contained 10 mM DTT. Data are presented as mean ± S.E. of three to seven independent experiments.

Oocyte Preparation and cRNA Injection—Oocytes were surgically removed from anesthetized *X. laevis* frogs, dissected, and defolliculated as described by Riedel *et al.* (30). In brief, for anesthesia tricaine methane sulfonate (Sigma) was used. The removed oocytes were separated by collagenase treatment (2 mg/ml) for 2 h. Healthy stage V-VI oocytes were manually selected and 25 ng of wild type or mutant cRNA were injected per oocyte. As control, water-injected oocytes were used. Injected oocytes were maintained at 19 °C in modified Barth's medium (5 mM HEPES/NaOH pH 7.4, 100 mM NaCl, 1 mM KCl, 1 mM $CaCl_2$, 1 mM $MgCl_2$, 10,000 units/ml penicillin, and 10 mg/ml streptomycin). 5–6 days after injection electrophysiological measurements or biochemical studies were performed.

Two-electrode Voltage Clamp Experiments—Two-electrode voltage clamp signals were recorded to assess the electrogenic function of the surface-expressed transport protein. Oocytes were placed in a flow-through chamber and continuously superfused (75 μl/s) with oocyte Ringer (ORi) buffer (10 mM MES/Tris, pH 6.5, 100 mM NaCl, 1 mM $MgCl_2$, 1 mM $CaCl_2$, 2 mM KCl) in the absence or presence of amino acids at a concentration of 20 mM. Quick and reproducible solution exchanges were achieved using a small tube-like chamber (0.1 ml) combined with fast superfusion (31, 32). Microelectrodes with resistances between 0.8 and 1.4 MΩ were pulled of borosilicate glass and filled with 3 M KCl. Whole-cell currents were recorded and filtered at 100 Hz using a two-electrode voltage clamp amplifier (OC-725C, Hamden) and sampled at 85 Hz. Oocytes were voltage clamped at a membrane potential of −60 mV. Currents induced by application of amino acids were calculated as the difference of the currents measured in the presence and absence of amino acid. All experiments were performed at room temperature (≈22 °C).

To determine the effect of the extracellular pH on hPAT1 function, the currents induced by 20 mM glycine at pH values varying from 5.0 to 8.0 (ORi buffer: 10 mM MES/Tris or HEPES/Tris, 100 mM NaCl, 1 mM $MgCl_2$, 1 mM $CaCl_2$, 2 mM KCl) were recorded. The Michaelis constants (K_t) were derived from experiments with seven different glycine concentrations (0–100 mM) at pH 6.5 in ORi buffer. Mean values ± S.E. were calculated from measurements of 6–8 oocytes from two batches and the kinetic constants were obtained by nonlinear regression of the Michaelis-Menten plot (SigmaPlot, Systat Software GmbH, Erkrath, Germany).

To assess the influence of DTT on transporter function oocytes were exposed to 10 mM DTT in modified Barth's medium (5 mM HEPES/NaOH pH 7.4, 100 mM NaCl, 1 mM KCl, 1 mM $CaCl_2$, 1 mM $MgCl_2$) for 20 min. Two-electrode voltage clamp experiments were performed as described above with the exception that all buffers contained 10 mM DTT.

Data were analyzed using the Superpatch 2000 program (Julius-Bernstein-Institute for Physiology, SP-Analyzer by T. Böhm, Halle, Germany). Statistical values are expressed as mean ± S.E. from measurements of 6–8 oocytes from at least two batches of oocyte preparation.

Immunofluorescence of Transfected HRPE Cells and cRNA-injected X. laevis Oocytes—Transfected HRPE cells grown on coverslips in 6-well plates were fixed and permeabilized with 4% paraformaldehyde and 0.05% Triton X-100 in phosphate-buffered saline (PBS) for 20 min. After removal of excess of paraformaldehyde by incubation with 0.1 mM NH_4Cl, nonspecific binding was blocked with 5% bovine serum albumin (BSA) in PBS. Cells were then incubated for 2 h with the primary antibody (rabbit anti-HA tag) diluted 1:2000 in 5% BSA/PBS, washed, and incubated for 1 h in the dark with the secondary antibody (goat anti-rabbit AlexaFluor® 488) diluted 1:500 in 5% BSA/PBS. Nuclei were stained with DAPI (4′,6-diamidino-2-phenylindole dihydrochloride; 1:100 in PBS). Coverslips were mounted on microscope slides using CitiFluor® (Plano, Wetzlar, Germany). All steps were performed at room temperature.

Oocytes expressing either wild type or mutant transporter were fixed with ethanol/acetic acid (95:5) for 1.5 h at 4 °C. After washing with 5% BSA/PBS several times, they were incubated overnight at 4 °C with the primary antibody (rabbit anti-HA tag) diluted 1:1600 in 5% BSA/PBS followed by incubation for 1 h at room temperature with the secondary antibody (goat anti-rabbit AlexaFluor® 488) 1:500 in 5% BSA/PBS. Oocytes were washed with 5% BSA/PBS and then mounted on microscope slides using CitiFluor® (Plano). Images were obtained using a confocal laser-scanning microscope (Nikon ECLIPSE TE2000).

Cell Surface Biotinylation of X. laevis Oocytes—For biotinylation of free extracellular cysteinyl sulfhydryl groups the membrane-impermeant reagent maleimide-PEG_{11}-biotin was used. In each case, 20 oocytes injected with either wild type or mutant transporter cRNA were incubated for 1 h at 4 °C in biotinylation reagent (0.5 mg/ml maleimide-PEG_{11}-biotin) in modified Barth's medium (5 mM HEPES/NaOH pH 7.4, 100 mM NaCl, 1 mM KCl, 1 mM $CaCl_2$, 1 mM $MgCl_2$). After washing with modified Barth's medium oocytes were homogenized in 20 μl/oocyte of lysis buffer (20 mM Tris/HCl, pH 7.4, 100 mM NaCl, 1% Triton X-100, 1x protease inhibitor (Roche Diagnostics GmbH, Mannheim, Germany)). The solubilized oocytes were then centrifuged at 16,000 × *g* (4 °C) for 15 min. To precipitate biotinylated proteins, 300 μl of the supernatant were added to 50 μl of NeutrAvidin® beads (Pierce) and incubated for 3 h at 4 °C. The beads were then washed three times with lysis buffer. For elution of bound protein, the lysis buffer was replaced by 30 μl of SDS-PAGE sample buffer (6 M urea, 100 mM Tris, pH 8.0, 0.02% bromphenol blue, 100 mM β-mercaptoethanol, 5% SDS, 15% glycerin) and heated to 95 °C for 10 min. Samples were analyzed by SDS-PAGE (10%, 8 × 10 cm) and immunoblotting.

SDS-PAGE of Alkylated Protein under Reducing and Nonreducing Conditions—Oocytes expressing either wild type or mutant hPAT1 were homogenized in 20 μl/oocyte of lysis buffer (20 mM Tris/HCl pH 7.4, 100 mM NaCl, 1% Triton X-100, 1× protease inhibitor). After centrifugation of solubilized oocytes (16,000 × *g*, 15 min, 4 °C) the supernatant was supplemented with 50 mM iodoacetamide and divided into two equal aliquots. To one sample, 100 mM DTT was added. Samples were analyzed by SDS-PAGE (7.5%, 10 × 10 cm) and immunoblotted in nonreducing sample buffer (8 M urea, 10% SDS, 100 mM Tris, pH 8.5, 0.02% bromphenol blue).

Immunoblotting of Oocyte Homogenates—Proteins were separated by SDS-PAGE and electrotransferred onto nitrocellulose membranes. After blocking of membranes in 5% nonfat dry milk in TBT buffer (50 mM Tris, pH 7.4, 150 mM NaCl, 0.2% Tween) for 1 h at room temperature, Western blots were probed with the primary antibody (mouse anti-HA tag) diluted 1:1000 in 5% nonfat dry milk in TBT buffer overnight at 4 °C. The secondary antibody (goat anti-mouse horseradish peroxidase-conjugated antibody) was used in a dilution of 1:2000 in 5% nonfat dry milk in TBT buffer for 1 h at room temperature. Antibody binding was detected by enhanced chemiluminescence with the Super Signal West Pico Substrate (Pierce).

RESULTS AND DISCUSSION

Functional Characterization of hPAT1 and HA-hPAT1 in X. laevis Oocytes—X. laevis oocytes were used for heterologous expression of wild type and mutant hPAT1/HA-hPAT1. To determine and characterize their transport function, oocytes were injected with transporter cRNA and the two-electrode voltage clamp technique was applied. As control, water-injected oocytes were used. Application of 20 mM glycine or proline to hPAT1-expressing oocytes at an extracellular pH of 6.5 and a membrane potential of −60 mV induced inward currents of 130 nA and 170 nA, respectively (Fig. 1*A*). L-Tryptophan, an inhibitor of hPAT1 transport function (33), did not induce detectable inward currents. In water-injected oocytes, glycine and proline were not able to generate inward currents. These results show that glycine and proline are transported by the human PAT1 expressed in oocytes in an electrogenic manner. As shown in Fig. 1*B*, the electrogenic uptake of glycine by hPAT1 and HA-hPAT1 is strongly pH-dependent. At pH 7.5 and 8.0, electrogenic uptake of glycine (20 mM) at a membrane potential of −60 mV was hardly detectable both at PAT1 and at HA-PAT1. With increasing extracellular H^+ concentrations the signals elicited by glycine increased with a maximum at pH 5.5 and 5.0. For determination of the kinetic constants of glycine uptake by hPAT1 and HA-hPAT1, glycine was added at increasing concentrations to hPAT1-expressing oocytes at pH 6.5 under voltage clamp conditions (membrane potential −60 mV) (Fig. 1*C*). The Michaelis constants obtained for the glycine transport were 11.4 ± 1.2 mM for hPAT1 and 12.4 ± 1.7 mM for HA-hPAT1. The transport characteristics of hPAT1 and HA-hPAT1 expressed in *X. laevis* oocytes correspond very well to previously published data on mouse and human PAT1 transport function (3, 33–35). Furthermore, these data show that the introduction of an HA tag at the N terminus of hPAT1 does neither alter the transport activity nor the apparent affinity of hPAT1-mediated transport. In addition, the HA tag does not change the substrate specificity as we have shown recently (6). For immunodetection in cells by fluorescence microscopy and by Western blot analysis HA-tagged constructs were used in subsequent transport studies and biochemical approaches.

Effect of DTT Treatment on Wild Type hPAT1 Transport Function—As an initial test for the existence of a functional relevant extracellular disulfide bond in hPAT1, we examined the effect of the reducing reagent DTT. The glycine induced inward currents in hPAT1-expressing oocytes and the L-[^{3}H]proline uptake in hPAT1-HRPE cells were both strongly inhibited by treatment with DTT (10 mM) for 20 min, respectively (Fig. 2). Under reducing conditions the transport of glycine in hPAT1-expressing oocytes was decreased by up to 85%. L-[^{3}H]Proline uptake in hPAT1-HRPE cells was inhibited by 60% compared with untreated cells. Incubation of wild type hPAT1 expressed either in *Xenopus* oocytes or HRPE cells with increasing concentrations of DTT led to a dose-dependent loss of transport function (data not shown). Consistently, we observed an inhibiting effect of DTT in two different expression systems indicating the existence of an extracellular disulfide bridge essential for full transport function. Fig. 3*A* shows the two-dimensional topology model of hPAT1. Assuming 11 transmembrane domains, three cysteine residues (Cys-180, Cys-329, and Cys-473) are located in the extracellular part of the membrane protein. Two of them, Cys-180 and Cys-329 are highly conserved and can be found in analogous positions in rat, mouse, and rabbit PAT1 and also in the paralogs hPAT2 and hPAT3 (Fig. 3*B*). Cys-473 is only present in the human PAT1. To identify the extracellular cysteine residues, which might be affected by DTT, single mutants were constructed by substituting each of the three cysteine residues with alanine or serine residue, respectively. If two cysteine residues are involved in disulfide bridge formation, mutation of either one of them should have an effect on transport function.

Functional Analysis of HA-hPAT1 Cysteine Mutants—Using the site-directed mutagenesis technique, six single point

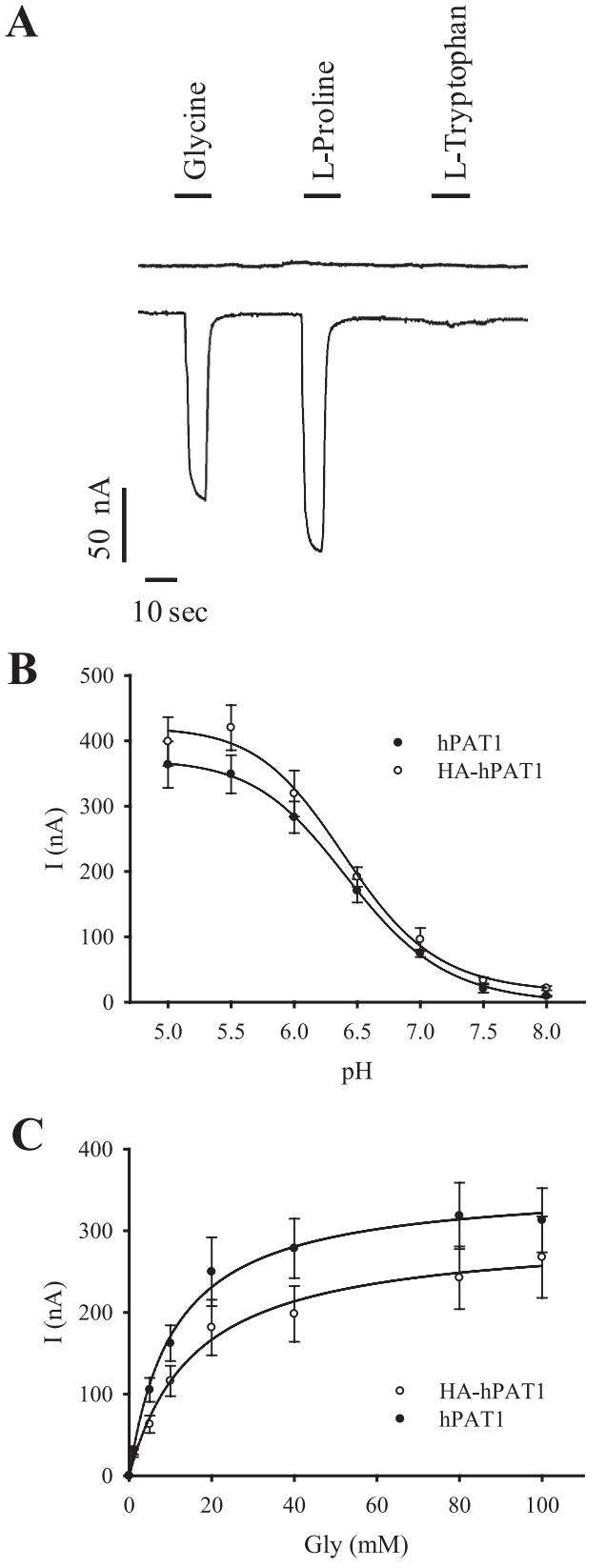

FIGURE 1. **Functional characterization of human PAT1 and HA-PAT1 expressed in *X. laevis* oocytes.** *A*, representative current traces of hPAT1-expressing oocytes in response to application of indicated amino acids (20 mM) in ORi buffer at pH 6.5. The *upper trace* shows a typical current recording of water-injected oocytes. *B*, oocytes expressing either hPAT1 or HA-hPAT1 were superfused with 20 mM glycine in ORi buffer at varying pH values. Current I was calculated as the difference of the currents measured in the presence and absence of glycine. Mean values ± S.E. from measurements of seven oocytes from two batches are shown. *C*, hPAT1- and HA-hPAT1-expressing oocytes were superfused with increasing concentrations of glycine in ORi buffer at pH 6.5. Mean ± S.E., $n = 6$ oocytes. Current I was calculated as the difference of the currents measured in the presence and absence of glycine. Kinetic constants were calculated by nonlinear regression of the Michaelis-Menten plot.

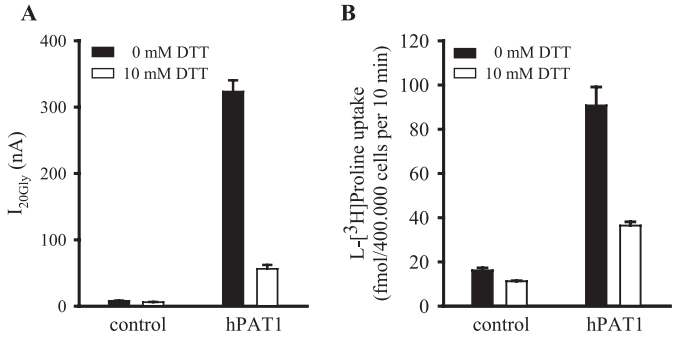

FIGURE 2. **Effect of DTT on hPAT1 function.** *A*, oocytes injected either with water (control) or hPAT1 cRNA (hPAT1) were incubated for 20 min at room temperature in Barth's medium with and without 10 mM DTT. The currents induced by 20 mM glycine at pH 6.5 were determined in the absence and presence (10 mM) of DTT. Currents (I_{20Gly}) were calculated as the difference of the currents measured in the presence and absence of glycine ($n = 6$ oocytes). *B*, HRPE cells transfected with empty vector pSPORT1 (control) or pSPORT1-hPAT1 (hPAT1) were treated with 10 mM DTT for 20 min at room temperature. Uptake of L-[^{3}H]proline (20 nM) was measured in the absence or presence (10 mM) of DTT at pH 6.0 for 10 min. Data are means ± S.E., $n = 4$.

mutants of HA-hPAT1 were generated. Each of the three extracellular cysteines (Cys-180, Cys-329, and Cys-473) was replaced by alanine or serine, respectively. The single mutants are designated C180A, C180S, C329A, C329S, C473A, and C473S. *Xenopus* oocytes were injected with wild type cRNA, mutant cRNA, or water as control and analyzed using the two-electrode voltage clamp technique. For mutants C180A, C180S, C329A, and C329S, the inward current induced by 20 mM glycine was significantly reduced. I_{20Gly} went up to only 13, 2, 27, and 17% of wild type HA-hPAT1 currents, respectively (Fig. 4*A*). In contrast, mutation of cysteine residue 473 had only a minor effect on I_{20Gly}. Mutants C473A and C473S displayed a glycine transport comparable to wild type HA-hPAT1.

Cysteine mutants and wild type HA-hPAT1 were also analyzed using the L-[^{3}H]proline uptake assay in cDNA-transfected HRPE cells. Mutants C180A/S and C329A/S displayed a dramatic loss of transport capability (Fig. 4*B*). L-[^{3}H]Proline uptake was reduced to 13, 12, 20, and 14% compared with wild type HA-hPAT1, respectively. This level corresponds to the degree of L-[^{3}H]proline uptake in cells transfected with the empty vector. Interestingly, uptake function was not affected by the mutation of cysteine 473. Both mutants, C473A and C473S transported L-[^{3}H]proline at levels comparable to wild type HA-hPAT1.

In *Xenopus* oocytes we could show that the replacement of the two highly conserved cysteine residues 180 and 329 either by an alanine or serine residue abolishes the transport function of hPAT1. The expression of wild type and mutant transporter in HRPE cells confirmed that the binding and/or transport of the substrate at the carrier was impaired in the respective mutants C180A/S and C329A/S. In contrast, exchanging the third extracellular nonconserved cysteine

A

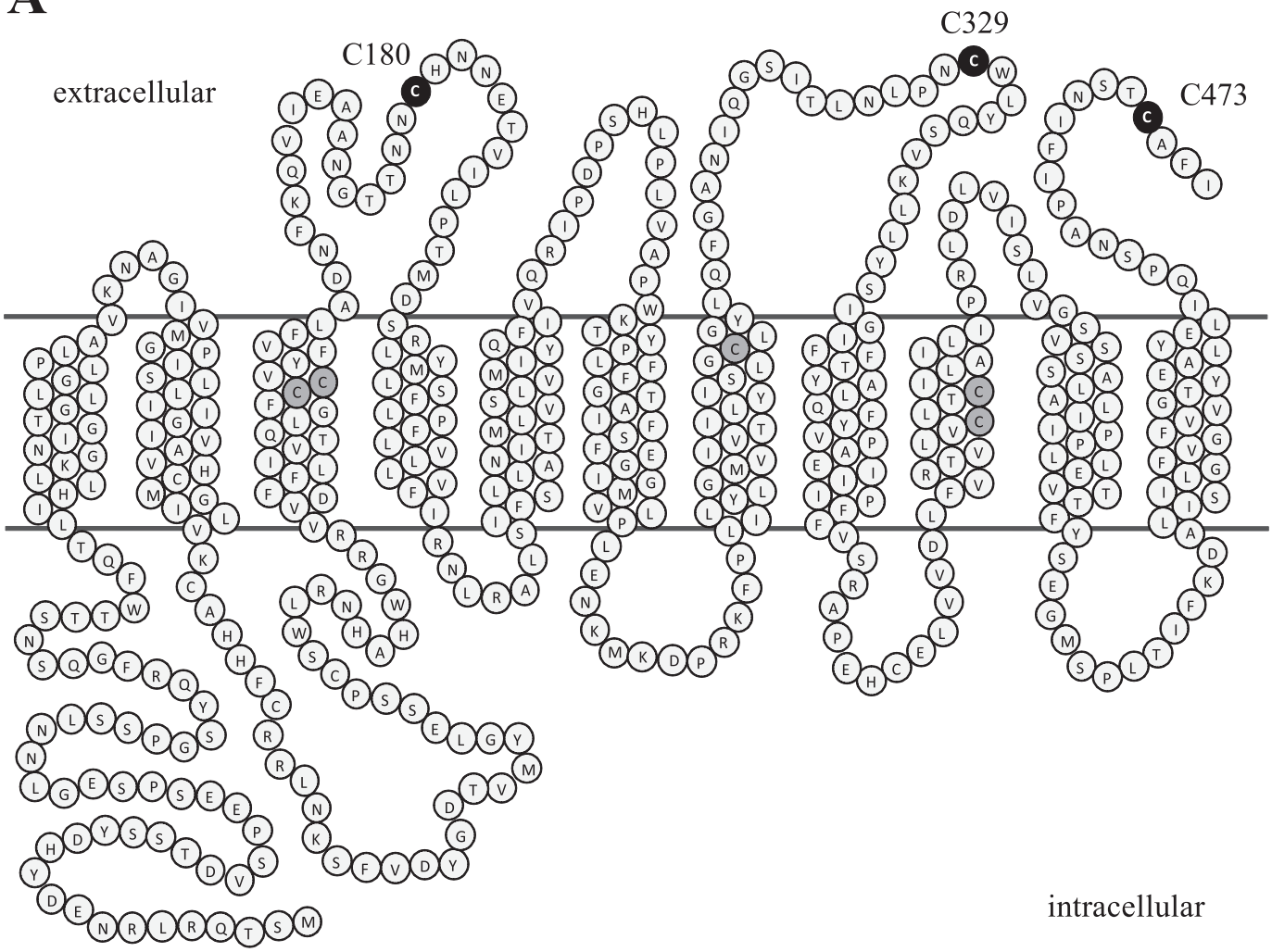

B

	extracellular loop 2	extracellular loop 4	C-terminus
	170 180 190	320 330 340	460 470
hPAT1	IEAANGTTNNCHNNETVILTP	GSITLNLPNCWLYQSVKLLYS	IQPSNAPIFINSTCAFI
rPAT1	IEAANGTTTNCNNNETVILTP	GSITLNLPNCWLYQSVKLLYS	IQPSHSDSSTNSTSAFI
mPAT1	IEAANGTTTNCNNNVTVIPTP	GSITLNLPNCWLYQSVKLLYS	IQPSHSDSSTNSTSAFI
rbPAT1	IEAANGTTSDCHNNETVVLTP	GSITLNLPNCWLYQSVKLLYS	IQPSNAPIFINSTSAYV
hPAT2	VEAVNSTTNNCYSNETVILTP	ASISLNLPNCWLYQSVKLLYI	LKSEDSHPFSNSTTFVR
hPAT3	VEEAHVTSNICQPREILTLTP	ASITLNLPNCWLYQSVKLMYS	LPQPISHSMANSTGVHA

FIGURE 3. **PAT1 amino acid sequence.** *A*, two-dimensional topology model of the 11 transmembrane structure of hPAT1. Extracellular cysteine residues mutated in this study (Cys-180, Cys-329, and Cys-473) are highlighted in *black*. Cysteine residues located in the transmembrane domains are highlighted in *gray*. *B*, partial amino acid sequence alignment of extracellular loops two and four and the C terminus of human PAT1 (hPAT1), rat PAT1 (rPAT1), mouse PAT1 (mPAT1), rabbit PAT1 (rbPAT1), hPAT2, and hPAT3. Cysteine residues 180, 329, and 473 in hPAT1 and analogous residues are *framed*.

residue 473 had no influence on transport function. These results indicate that Cys-180 and Cys-329 are essential for substrate transport either individually or by forming a disulfide bond. To investigate possible mistargeting, instability, and subsequent decreases in cell surface expression as known consequences of mutation in membrane proteins (17,

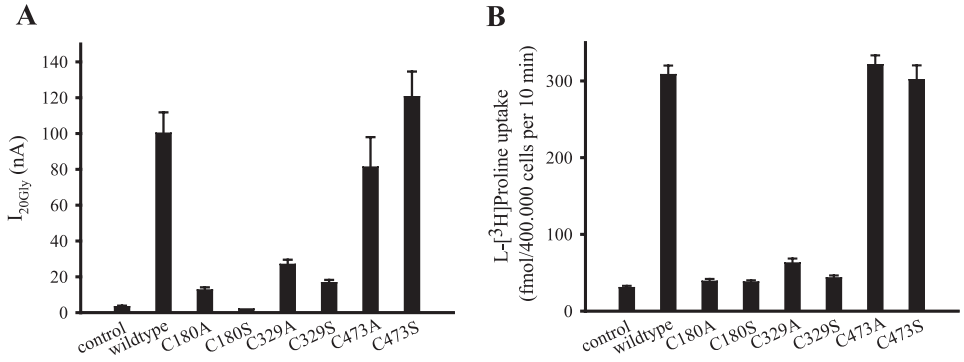

FIGURE 4. **Transport function of wild type HA-hPAT1 and cysteine mutants.** *A*, two-electrode voltage clamp recordings of oocytes injected either with wild type (HA-hPAT1) or mutant HA-hPAT1 cRNA. Water-injected oocytes were used as control. Inward currents induced by 20 mM glycine were determined at pH 6.5. Currents (I_{20Gly}) were calculated as the difference of the currents measured in the presence and absence of glycine. Mean values ± S.E. from measurements of 5 to 6 oocytes are shown. *B*, uptake of L-[^{3}H]proline (20 nM, 10 min, pH 6.0) was determined in HRPE cells transfected with pSPORT1-HA-hPAT1 (wild type) or the mutant HA-tagged hPAT1 cDNAs in pSPORT1. HRPE cells transfected with the empty vector pSPORT1 served as control. Data are means ± S.E., $n = 3–7$.

18), we examined the cell surface expression of wild type and mutant HA-hPAT1.

Cellular Localization of Wild Type and Mutant HA-hPAT1—For localization of wild type and mutant HA-hPAT1 expressed in *Xenopus* oocytes immunofluorescence was analyzed by confocal laser-scanning microscopy. cRNA-injected oocytes were probed with the primary rabbit anti-HA tag antibody. As shown in Fig. 5*A*, all mutant proteins were detected in the plasma membrane at similar levels as the wild type protein, except mutant C180S. The much weaker staining of C180S mutant in the plasma membrane, indicating a decrease in cell surface expression, could be the explanation for the loss of function of this single mutant. However, replacing the cysteine at the same position with an alanine resulted in a mutant protein, which reached the plasma membrane. A similar phenomenon has been described by Karnik *et al.* (36) for the G-protein-coupled receptor rhodopsin. They demonstrated that replacement of conserved cysteine residues in rhodopsin with serine caused detrimental effects on receptor folding and stability, probably due to the hydrophilic nature of the serine side chain. Interestingly, the analogous alanine mutants behaved like the wild type receptor. In cDNA- transfected HRPE cells expressing either wild type or mutant HA-hPAT1, incubation with a rabbit anti-HA tag antibody led to intense staining of the plasma membrane, indicating a wild type-like localization of all cysteine mutants (Fig. 5*B*). HRPE cells transfected with empty vector pSPORT1 served as control and showed only weak background fluorescence. The data of both experiments demonstrate very clearly that the low levels of transport activity of C180A/S and C329A/S mutants observed in cRNA-injected oocytes and cDNA-transfected HRPE cells were not caused by alterations of transporter protein levels in the plasma membrane. Hence the postulated disulfide bridge is not essential for the protein to reach or keep its cellular destination but rather plays a direct role in transport function.

Cell Surface Biotinylation of HA-hPAT1 Wild Type and Cysteine Mutants—To obtain further evidence for the existence of a disulfide bond between Cys-180 and Cys-329 in the extracellular part of PAT1, the membrane-impermeable thiol-reactive reagent maleimide-PEG_{11}-biotin was employed. To detect free accessible cysteine residues in wild type and mutant HA-hPAT1, cRNA-injected oocytes were incubated with maleimide-PEG_{11}-biotin, and the lysates were applied to neutravidin beads. In the wild type protein, there are three putative extracellular cysteine residues. Assuming the presence of an intramolecular disulfide bridge, the incubation with maleimide-PEG_{11}-biotin should result in biotin labeling of the third cysteine residue provided that it is not engaged in an intermolecular disulfide bridge. In the single cysteine mutants a disulfide bond between the remaining two cysteines would prevent labeling. Fig. 6 shows the Western blot analysis after biotinylation of wild type and cysteine mutants C180A, C329A, and C473A. The broad band at ~100 kDa probably corresponds to dimers and trimers resulting from aggregation, whereas the lower molecular mass band at 55 kDa represents the hPAT1 monomer. The high molecular aggregates most likely result from sample preparation. Detaching the biotin-protein complex from the neutravidin beads by heat is the crucial step. As hydrophobic interactions are intensified at higher temperatures, this inevitable treatment might trigger aggregation of membrane proteins to a different extent.

As expected, the wild type HA-hPAT1 was labeled by maleimide-PEG_{11}-biotin and could be detected in the eluate of a neutravidin pulldown experiment (Fig. 6*B*). Biotinylation of a free cysteine residue was also detected for the mutants C180A and C329A. In contrast, no coupling to biotin could be observed for mutant C473A, suggesting inaccessibility of Cys-180 and Cys-329 or a disulfide bond between both cysteines. To exclude the first scenario, oocytes expressing the mutant C473A were incubated with 10 mM DTT for 20 min prior to biotinylation with maleimide-PEG_{11}-biotin. In Fig. 6*C* the Western blot analysis of the eluate of corresponding neutravidin pulldown experiments shows that mutant C473A could be biotinylated after pretreatment with DTT, indicating that cysteine residues Cys-180 and Cys-329 are in principle accessible for the biotinylation reagent. Thus, the apparent absence of a free sulfhydryl group in mutant C473A strongly suggests a disulfide bridge linkage of Cys-180 and Cys-329. Furthermore, the labeling of the wild type transporter excludes the existence of an intermolecular disulfide bridge.

SDS-PAGE under Reducing and Nonreducing Conditions—The mobility of wild type and mutant protein analyzed on a 7.5% SDS gel under reducing (+DTT) and nonreducing (−DTT) conditions was examined. Lysates of oocytes expressing either wild type or mutant HA-hPAT1 were alkylated and supplemented with or without 100 mM DTT. As shown in Fig. 7, the wild type transporter HA-hPAT1 migrated faster under

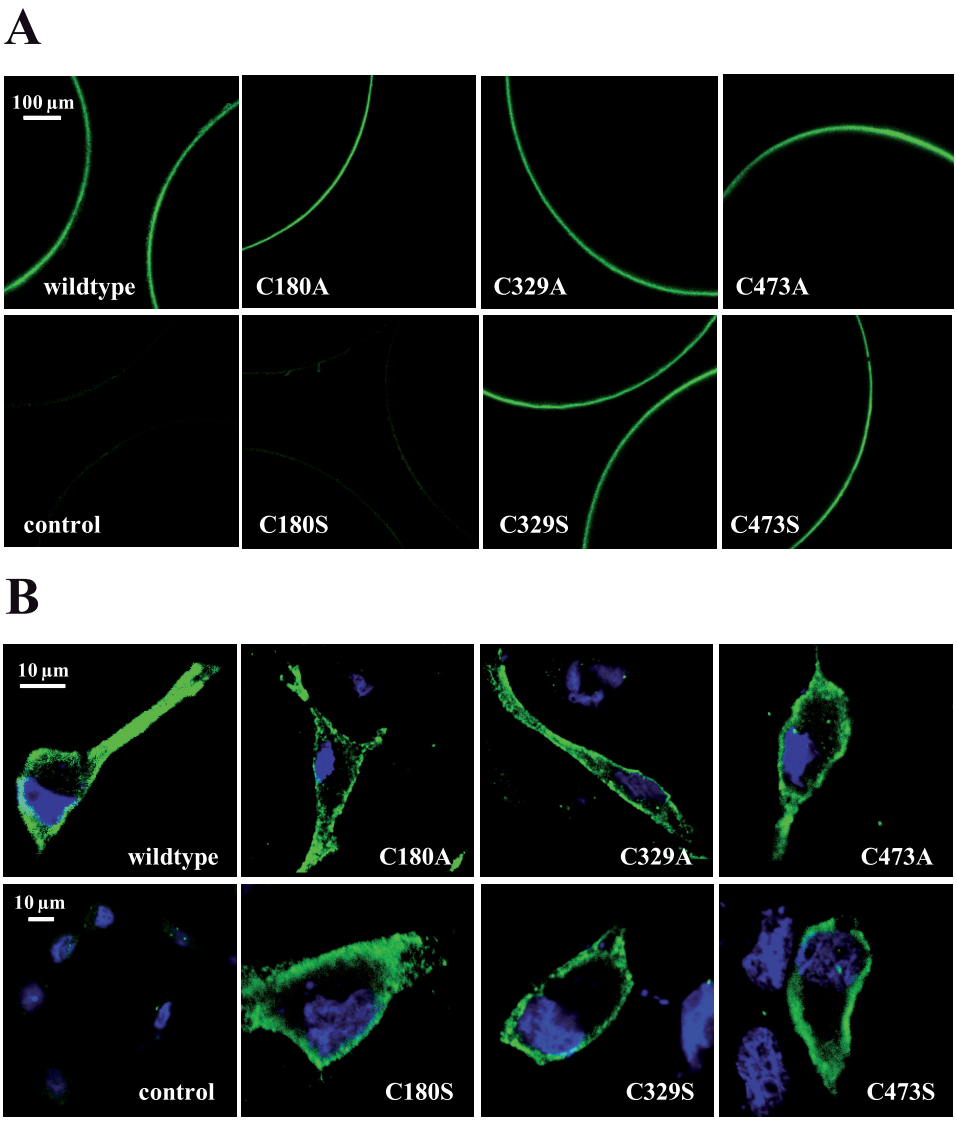

FIGURE 5. **Localization of immunostained HA-hPAT1 (wild type) and cysteine mutants expressed in *X. laevis* oocytes and HRPE cells detected by confocal laser-scanning microscopy.** *A*, oocytes were injected either with water (control) or cRNAs of wild type and mutant HA-hPAT1. Five days after injection oocytes were incubated with the primary rabbit anti-HA tag antibody followed by the secondary goat anti-rabbit AlexaFluor® 488 antibody. *B*, HRPE cells transfected either with the empty vector pSPORT1 (control) or with the vector containing wild type HA-hPAT1 or mutant HA-hPAT1 cDNA as indicated were incubated with the primary rabbit anti-HA tag antibody followed by the secondary goat anti-rabbit AlexaFluor® 488 antibody. Nuclei were stained with DAPI.

nonreducing than under reducing conditions. This behavior, probably caused by a more compact state of the protein is a hint for the presence of a disulfide bond in HA-hPAT1 leading to a denser packaging. For mutants C180A and C329A there is no difference in gel mobility under reducing or nonreducing conditions. The protein bands correspond to wild type protein under reducing conditions, indicating the loss of the putative disulfide bond in both mutants. Mutant C473A migrated faster under nonreducing conditions than under reducing conditions as observed for the wild type protein, which again implies the existence of a disulfide bond between Cys-180 and Cys-329. These results confirm the presence of a disulfide bond between the highly conserved extracellular cysteine residues Cys-180 and Cys-329, which can be disrupted by either 100 mM DTT or a point mutation (C180A and C329A).

Cell Surface Biotinylation of a Triple Cysteine Mutant—Biotinylation experiments and protein mobility assays both show very clearly that Cys-180 and Cys-329 are involved in forming a disulfide bridge. Nevertheless the data do not exclude *per se* the possibility that these cysteine residues might form a disulfide bond with a cysteine residue located at the extracellular end of the transmembrane domains, rather than with each other. In the amino acid sequence of hPAT1, there are five additional cysteine residues present in putative transmembrane domains 3, 7, and 9 (Fig. 3). To rule out that one of them is involved in disulfide formation, we generated a triple cysteine mutant of HA-hPAT1 where all three extracellular cysteine residues were removed simultaneously. This mutant was designated C180/329/473A. Next, the triple mutant was expressed in *X. laevis* oocytes and subjected to biotinylation experiments using the membrane-impermeable thiol-reactive reagent maleimide-PEG_{11}-biotin. As shown in Fig. 8, biotin labeling of free cysteine residues could only be detected for the wild type transporter. In contrast, for the triple mutant no band could be detected in the eluate of neutravidin pulldown experiments. To exclude that the lack of labeling is caused by a reduced plasma membrane expression, the expression of the mutant was analyzed by confocal laser-scanning microscopy. The detected immunofluorescence of the triple mutant was comparable to wild type transporter, indicating a wild type-like membrane expression (data not shown). The absence of free sulfhydryl groups in the triple mutant shows very clearly that the cysteine residues in the transmembrane domains are not accessible and therefore no potential partners for disulfide bridges.

In summary, specific transport activity of wild type hPAT1 was inhibited in the presence of the disulfide bond reducing agent DTT in two different expression systems. This implies that a disulfide bond is formed and can be reduced. Expression of wild type and mutant transporters in *Xenopus* oocytes and HRPE cells showed that mutants C180A/S and C329A/S were not able to bind and transport the typical substrates glycine and proline, respectively. Substitution of the two highly conserved cysteine residues Cys-180 and Cys-329 either by alanine or serine residues thus led to a loss of function, underlining their

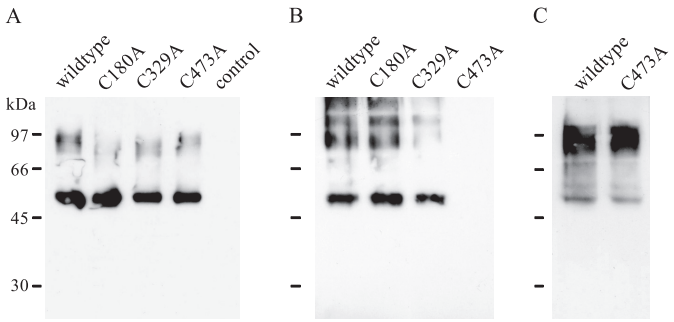

FIGURE 6. **Western blot analysis of cell surface biotinylation of free sulfhydryl groups using maleimide-PEG_{11}-biotin.** *A*, lysates of biotinylated oocytes expressing either wild type or mutant HA-hPAT1. As control, water-injected oocytes were used. *B*, eluates of neutravidin beads incubated with lysates shown in *A*. *C*, eluate of neutravidin beads incubated with lysate of biotinylated oocytes expressing wild type or mutant C473A HA-hPAT1 preincubated for 20 min with 10 mM DTT prior to biotinylation with maleimide-PEG_{11}-biotin. For immunodetection, samples were separated on a 10% SDS gel (8 × 10 cm) followed by incubation with the mouse anti-HA tag antibody.

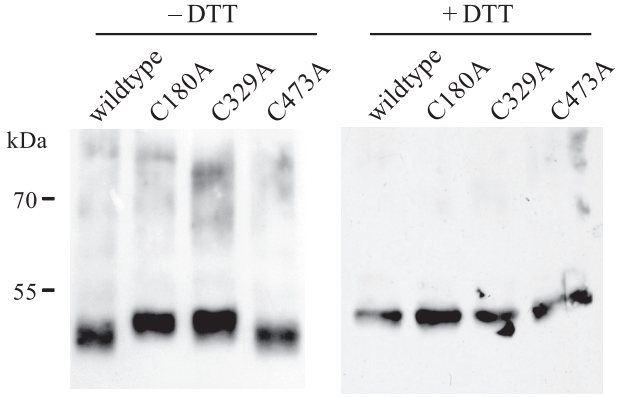

FIGURE 7. **Western blot analysis of SDS-PAGE of wild type and mutant HA-hPAT1 protein under nonreducing (−DTT) and reducing (+DTT) conditions.** Lysates of oocytes expressing either wild type or mutant transporter were alkylated and separated under reducing (100 mM DTT) or nonreducing (0 mM DTT) conditions on a 7.5% SDS gel (10 × 10 cm), followed by immunodetection with the mouse anti-HA tag antibody.

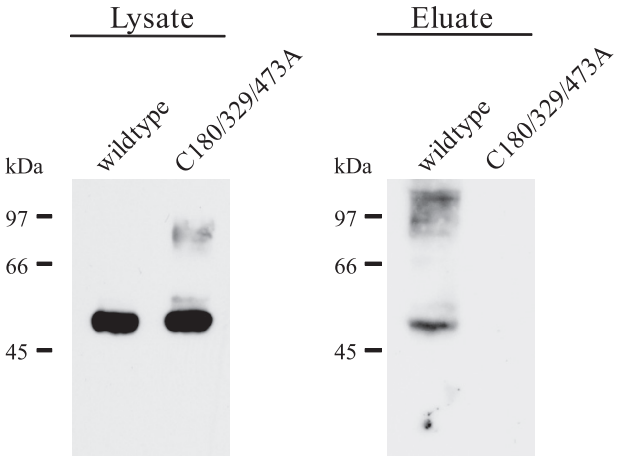

FIGURE 8. **Western blot analysis of cell surface biotinylation of free sulfhydryl groups using maleimide-PEG_{11}-biotin.** Oocytes were injected with cRNAs of wild type and triple mutant HA-hPAT1. Lysates of biotinylated oocytes were incubated with neutravidin beads. For elution, the beads were heated to 95 °C in sample buffer. For immunodetection samples were separated on a 10% SDS gel (8 × 10 cm) followed by incubation with the mouse anti-HA tag antibody.

functional or structural importance individually or as parts of a disulfide bridge. In contrast, mutants C473A/S showed a transport activity comparable to wild type hPAT1. Immunofluorescence studies demonstrated that the loss of function of the mutant transporters was not caused by a mislocalization of the protein within the cell. Biochemical approaches like biotinylation of free sulfhydryl groups using maleimide-PEG_{11}-biotin and protein mobility assays on SDS-PAGE under reducing and nonreducing conditions provide additional evidence for the existence of a disulfide bond between Cys-180 and Cys-329. This disulfide bridge linkage of extracellular loop (EL) 2 and EL 4 is therefore essential for transport function of hPAT1 but not for membrane localization.

According to the 11 transmembrane domain model of hPAT1 (37), cysteine residues Cys-180 and Cys-329 are located in the extracellular part of the protein. Assuming a nine transmembrane domain topology of hPAT1 (4), both cysteines would be located in the cytoplasmatic loops and could not form a disulfide bond. Our results support the 11 transmembrane domain model for hPAT1.

This study provides the first information about the putative three-dimensional conformation of hPAT1. The loss of a disulfide bond has a dramatic effect on transporter structure rendering it unable to transport its substrates, confirming once again the key role of disulfide bonds in stabilizing the three-dimensional structure of a protein. The importance of cysteine residues for the structural integrity and functionality of membrane proteins has been established for many GPCRs (38, 39) but for only very few transporters (17, 25). In case of hPAT1 a disulfide bond between Cys-180 in the EL 2 and C329 in EL 4 would lead to a close proximity of these loops and furthermore transmembrane segments 3, 4, 7, and 8. The covalently linked assembly of structures distant from each other in the primary structure could be involved in forming or stabilizing the putative substrate binding pocket and translocation pore.

Acknowledgments—We thank Prof. Schmalzing (RWTH, Aachen, Germany) for providing the oocyte expression vector pNKS-transducin. We also thank Dr. Manuela Klapperstück and Dr. Wolfgang Boldt (Julius-Bernstein-Institute for Physiology, Halle, Germany) for an introduction to oocyte techniques and helpful advice. The authors thank Monika Schmidt (Julius-Bernstein-Institute for Physiology) for excellent technical assistance.

REFERENCES

1. Fredriksson, R., Nordström, K. J., Stephansson, O., Hägglund, M. G., and Schiöth, H. B. (2008) *FEBS Lett.* **582,** 3811–3816
2. Sagné, C., Agulhon, C., Ravassard, P., Darmon, M., Hamon, M., El Mestikawy, S., Gasnier, B., and Giros, B. (2001) *Proc. Natl. Acad. Sci. U.S.A.* **98,** 7206–7211
3. Boll, M., Foltz, M., Rubio-Aliaga, I., Kottra, G., and Daniel, H. (2002) *J. Biol. Chem.* **277,** 22966–22973
4. Chen, Z., Fei, Y. J., Anderson, C. M., Wake, K. A., Miyauchi, S., Huang, W., Thwaites, D. T., and Ganapathy, V. (2003) *J. Physiol* **546,** 349–361
5. Thwaites, D. T., McEwan, G. T., Cook, M. J., Hirst, B. H., and Simmons, N. L. (1993) *FEBS Lett.* **333,** 78–82
6. Metzner, L., Natho, K., Zebisch, K., Dorn, M., Bosse-Doenecke, E., Ganapathy, V., and Brandsch, M. (2008) *Biochim. Biophys. Acta* **1778,** 1042–1050
7. Anderson, C. M., Grenade, D. S., Boll, M., Foltz, M., Wake, K. A., Kennedy,

D. J., Munck, L. K., Miyauchi, S., Taylor, P. M., Campbell, F. C., Munck, B. G., Daniel, H., Ganapathy, V., and Thwaites, D. T. (2004) *Gastroenterology* **127,** 1410–1422
8. Metzner, L., Kalbitz, J., and Brandsch, M. (2004) *J. Pharmacol. Exp. Ther.* **309,** 28–35
9. Brandsch, M. (2006) *Amino Acids* **31,** 119–136
10. Thwaites, D. T., and Anderson, C. M. (2007) *Biochim. Biophys. Acta* **1768,** 179–197
11. Larsen, M., Larsen, B. B., Frølund, B., and Nielsen, C. U. (2008) *Eur. J. Pharm. Sci.* **35,** 86–95
12. Bröer, S., Bailey, C. G., Kowalczuk, S., Ng, C., Vanslambrouck, J. M., Rodgers, H., Auray-Blais, C., Cavanaugh, J. A., Bröer, A., and Rasko, J. E. (2008) *J. Clin. Invest.* **118,** 3881–3892
13. Chen, J. G., Liu-Chen, S., and Rudnick, G. (1997) *Biochemistry* **36,** 1479–1486
14. Sur, C., Schloss, P., and Betz, H. (1997) *Biochem. Biophys. Res. Commun.* **241,** 68–72
15. Chen, R., Wei, H., Hill, E. R., Chen, L., Jiang, L., Han, D. D., and Gu, H. H. (2007) *Mol. Cell Biochem.* **298,** 41–48
16. Turner, R. J., and George, J. N. (1983) *J. Biol. Chem.* **258,** 3565–3570
17. Gagnon, D. G., Bissonnette, P., and Lapointe, J. Y. (2006) *J. Gen. Physiol.* **127,** 145–158
18. Lambert, G., Traebert, M., Biber, J., and Murer, H. (2000) *J. Membr. Biol.* **176,** 143–149
19. Wakabayashi, K., Nakagawa, H., Tamura, A., Koshiba, S., Hoshijima, K., Komada, M., and Ishikawa, T. (2007) *J. Biol. Chem.* **282,** 27841–27846
20. Jess, U., Betz, H., and Schloss, P. (1996) *FEBS Lett.* **394,** 44–46
21. Kage, K., Fujita, T., and Sugimoto, Y. (2005) *Cancer Sci.* **96,** 866–872
22. Hebert, D. N., and Carruthers, A. (1991) *Biochemistry* **30,** 4654–4658
23. Zottola, R. J., Cloherty, E. K., Coderre, P. E., Hansen, A., Hebert, D. N., and Carruthers, A. (1995) *Biochemistry* **34,** 9734–9747
24. Pajor, A. M., Krajewski, S. J., Sun, N., and Gangula, R. (1999) *Biochem. J.* **344,** 205–209
25. Henriksen, U., Fog, J. U., Litman, T., and Gether, U. (2005) *J. Biol. Chem.* **280,** 36926–36934
26. Sturm, A., Gorboulev, V., Gorbunov, D., Keller, T., Volk, C., Schmitt, B. M., Schlachtbauer, P., Ciarimboli, G., and Koepsell, H. (2007) *Am. J. Physiol. Renal Physiol* **293,** F767–F779
27. Asaka, J., Terada, T., Tsuda, M., Katsura, T., and Inui, K. (2007) *Mol. Pharmacol.* **71,** 1487–1493
28. Dorn, M., Jaehme, M., Weiwad, M., Markwardt, F., Rudolph, R., Brandsch, M., and Bosse-Doenecke, E. (2009) *FEBS Lett.* **583,** 1631–1636
29. Blakely, R. D., Clark, J. A., Rudnick, G., and Amara, S. G. (1991) *Anal. Biochem.* **194,** 302–308
30. Riedel, T., Lozinsky, I., Schmalzing, G., and Markwardt, F. (2007) *Biophys. J.* **92,** 2377–2391
31. Klapperstück, M., Büttner, C., Böhm, T., Schmalzing, G., and Markwardt, F. (2000) *Biochim. Biophys. Acta* **1467,** 444–456
32. Bretschneider, F., and Markwardt, F. (1999) *Methods Enzymol.* **294,** 180–189
33. Metzner, L., Kottra, G., Neubert, K., Daniel, H., and Brandsch, M. (2005) *FASEB J.* **19,** 1468–1473
34. Boll, M., Foltz, M., Anderson, C. M., Oechsler, C., Kottra, G., Thwaites, D. T., and Daniel, H. (2003) *Mol. Membr. Biol.* **20,** 261–269
35. Foltz, M., Mertl, M., Dietz, V., Boll, M., Kottra, G., and Daniel, H. (2005) *Biochem. J.* **386,** 607–616
36. Karnik, S. S., Sakmar, T. P., Chen, H. B., and Khorana, H. G. (1988) *Proc. Natl. Acad. Sci. U.S.A.* **85,** 8459–8463
37. Boll, M., Foltz, M., Rubio-Aliaga, I., and Daniel, H. (2003) *Genomics* **82,** 47–56
38. Frändberg, P. A., Doufexis, M., Kapas, S., and Chhajlani, V. (2001) *Biochem. Biophys. Res. Commun.* **281,** 851–857
39. Cook, J. V., and Eidne, K. A. (1997) *Endocrinology* **138,** 2800–2806